LETTER TO THE EDITOR

Expanded clinical, genetic, and biological spectrum of filaminopathies with hematological involvement

Authors

Charlotte Brillon,[1,2] Marjorie Poggi,[2] Mathieu Fiore,[3] Cyril Goizet,[4] Sophie Bayart,[5] Mélanie Y. Daniel,[6] Jean-Baptiste Valentin,[7] Nathalie Hezard,[8] Johannes Van Agthoven,[9] Véronique Sbarra,[2] Marie Loosveld,[8] Céline Falaise,[1,10] Marie-Christine Alessi,[2,10] Manal Ibrahim-Kosta,[2,10] and Paul Saultier[1,2,10]

[1]Department of Pediatric Hematology, Immunology and Oncology, Aix Marseille University, APHM, La Timone Children's Hospital, Marseille, France; [2]Aix-Marseille Univ, INSERM, INRAE, C2VN, Marseille, France; [3]Department of Hematology, Reference Center for Inherited Platelet Disorders, University of Bordeaux, University Hospital of Bordeaux, INSERM, U1034, Pessac, France; [4]Department of Genetics, Reference Center for Neurogenetics, University Hospital of Bordeaux, Bordeaux, France; [5]Reference Center for Hemophila and other Coagulation Factors Deficiency, Reference Center for Inherited Platelet Disorders and von Willebrand's Disease, University Hospital of Rennes, France; [6]Hematology and Transfusion Department, French National Institute for Health and Medical Research, University Hospital of Lille, Pasteur Institute of Lille, University of Lille, U1011-European Genomic Institute for Diabetes, Lille, France; [7]Hemophilia Treatment Center, University Hospital of Tours, Tours, France; Hematology Laboratory, CHU Timone, Marseille, France; [9]Structural Biology Program, Division of Nephrology/Department of Medicine, Massachusetts General Hospital and Harvard Medical School, Charlestown, MA, USA and [10]APHM, CHU Timone, French Reference Center on Inherited Platelet Disorders, Marseille, France

Correspondence:
M. POGGI - marjorie.poggi@univ-amu.fr

https://doi.org/10.3324/haematol.2025.288445

Received: June 17, 2025.
Accepted: October 1, 2025.
Early view: October 9, 2025.

Supplemental Table

Table S1: Genetic characteristics and prediction of pathogenicity for both null and missense *FLNA* variants.

	Patient	Variant DNA	Variant protein	gnomAD exome v.4 frequency	CADD score	ACMG	MPA score
Null variants	**P1** **P2**	exon2:c.133C>T	p.Gln45Ter	*	37	5	10 (nonsense)
	P3	exon 4: c.639G>A	p.Trp213Ter	*	36	5	10 (nonsense)
	P4 **P5**	exon7:c.1056delG	p.Thr353LeufsTer32	*	*	5	10 (frameshift)
	P6	exon8:c.1120_1125delinsTCTTG	p.Val374SerfsTer2	*	*	5	10 (frameshift)
	P7	exon13:c.1835C>A	p.Ser612Ter	*	39	5	10 (nonsense)
	P8	exon22:c.3677_3684del	p.Pro1226LeufsTer38	*	*	5	10 (frameshift)
	P9	exon31:c.5027_5030del	p.Thr1676ArgfsTer8	*	*	5	10 (frameshift)
	P10	exon31:c.5146dup	p.Gln1716ProfsTer77	*	*	5	10 (frameshift)
	P11	intron16:c.2404+1del		*	*	5	10 (high splice)
	P12	Duplication of exons 2 to 29				5	
Missense variants	**P13**	exon3:c.568C>T	p.Arg190Trp	$2.7x10^{-6}$	23	3	9 (high missense)
	P14	exon9:c.1354G>A	p.Gly452Ser	$9.1x10^{-7}$	25	3	10 (high missense)
	P15	exon22:c.3755C>T	p.Ala1252Val	$2.6x10^{-5}$	24	3	9 (high missense)
	P16	exon31 :c.5053A>G	p.Thr1685Ala	*	24	3	10 (high missense)
	P17	exon39 :c.6372C>G	p.His2124Gln	$9.1x10^{-7}$	24	3	10 (high missense)
	P18	exon42:c.6791G>A	p.Arg2264Gln	$9.1x10^{-7}$	26	3	10 (high missense)

Variant nomenclature follows the Human Genome Variation Society (HGVS) recommendations.
Reference sequences used: NM_001110556.2 and NP_001104026.1.
ACMG classification : (3) uncertain significance and (5) pathogenic. * : no match

Table S1: Genetic characteristics and prediction of pathogenicity for both null and missense *FLNA* variants. The frequency of each variant in general populations was determined using GnomAD exome v4. No matches were found for null variants while five missense variants were rarely reported. The variants were classified according to the ACMG (American College of Medical Genetics) guidelines. Different scores were used to predict the pathogenicity of the variants, including the CADD score (Combined Annotation Dependant Depletion) and the MPA score (MoBiDiC Prioritization Algorithm). All null variants were classified as pathogenic (class 5) based on the ACMG guidelines. All missense variants were classified as of “uncertain significance” (class 3).

Supplemental references

1. Lad Y, Kiema T, Jiang P, et al. Structure of three tandem filamin domains reveals auto-inhibition of ligand binding. EMBO J 2007;26(17):3993–4004.

2. Liu J, Lu F, Ithychanda SS, et al. A mechanism of platelet integrin αIIbβ3 outside-in signaling through a novel integrin αIIb subunit–filamin–actin linkage. Blood 2023;141(21):2629–2641.

Supplemental Figures Legends

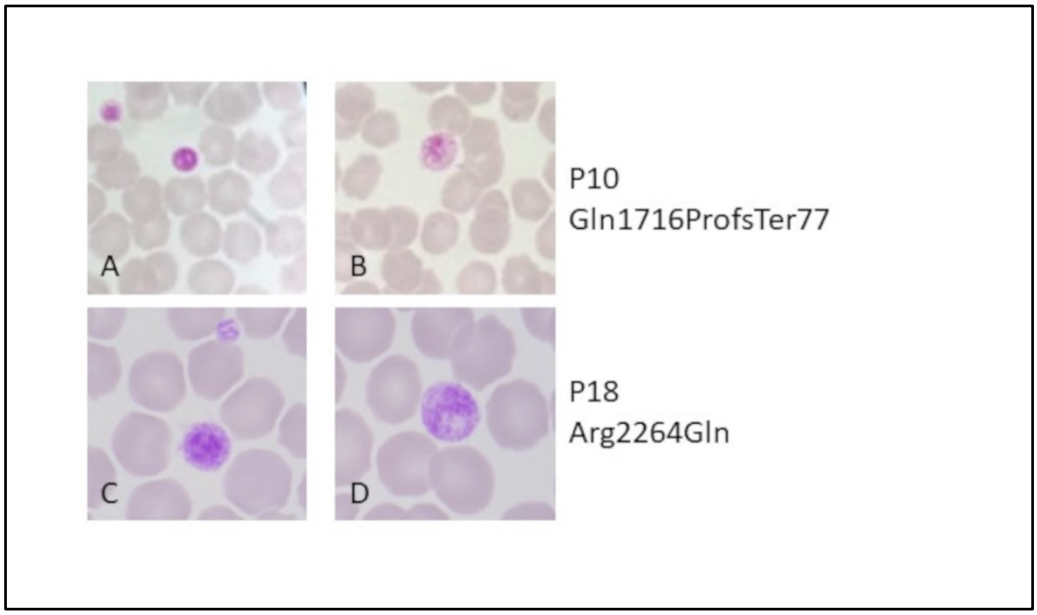

Figure S1 : Platelet morphology evaluated by light microscopy. Smears were stained with May-Grünwald Giemsa. A. and B. show large and giant platelets from P10. C and D. show large and giant platelets from P18.

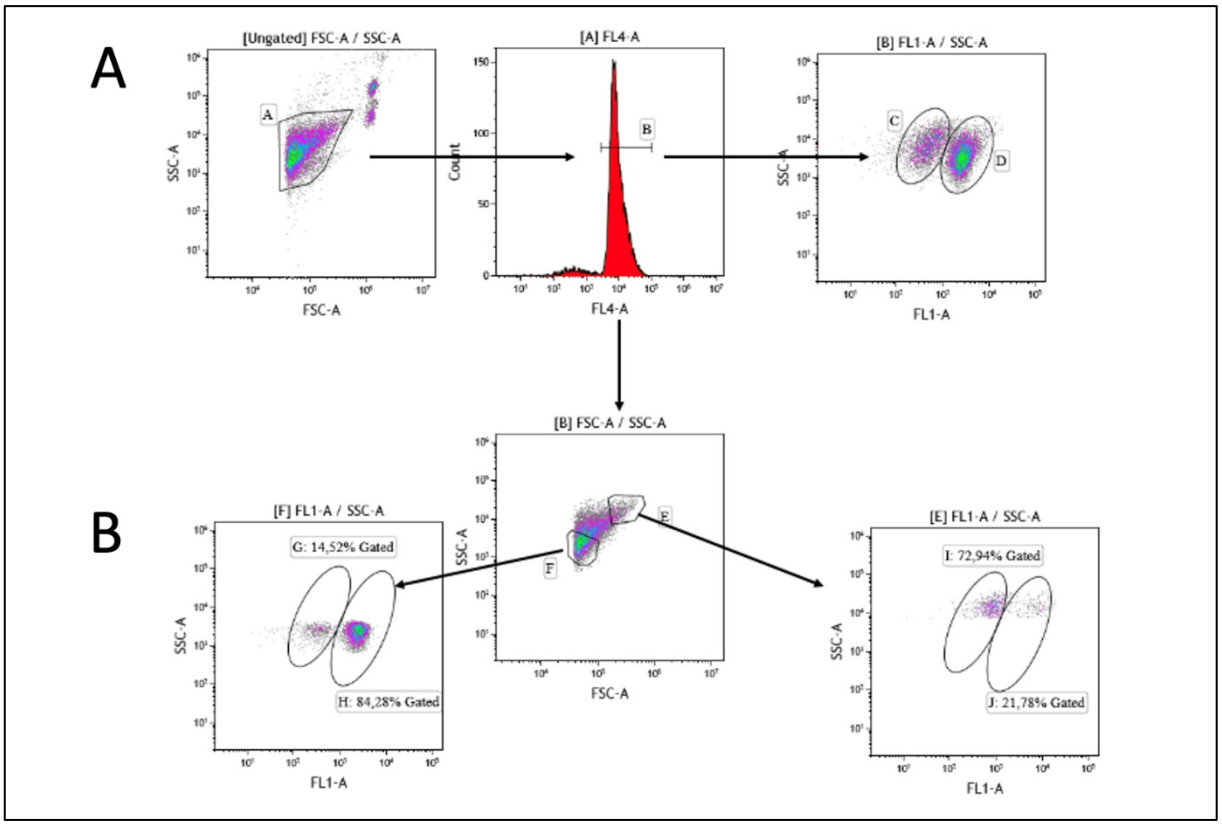

Figure S2: Supplemental files about flow cytometry measurements (FCM). (A) FCM gating strategy. This strategy was used to isolate platelets from fixed blood samples, allowing for the exclusive analysis of the platelet population. First, cells were gated based on their structural and morphological characteristics [first panel, forward scatter/side scatter (FSC/SSC), gate A]. Then, platelets expressing CD41 were selected from gate A (second panel, gate B). The third panel shows two platelet subpopulations isolated from gate B: FLNA-negative platelets (gate C, left) and FLNA-positive platelets (gate D, right). FL4 corresponds to the APC channel, which detects CD41, while FL1 corresponds to the AF488 channel, which detects FLNA. **(B) FLNA-negative platelets are larger than platelet containing FLNA.** Gate E represents the subpopulation of larger platelets in the patient, in which 72% of platelets are FLNA-negative. Gate F focuses on the subpopulation of smaller-sized platelets, which contains 84% FLNA-positive platelets.

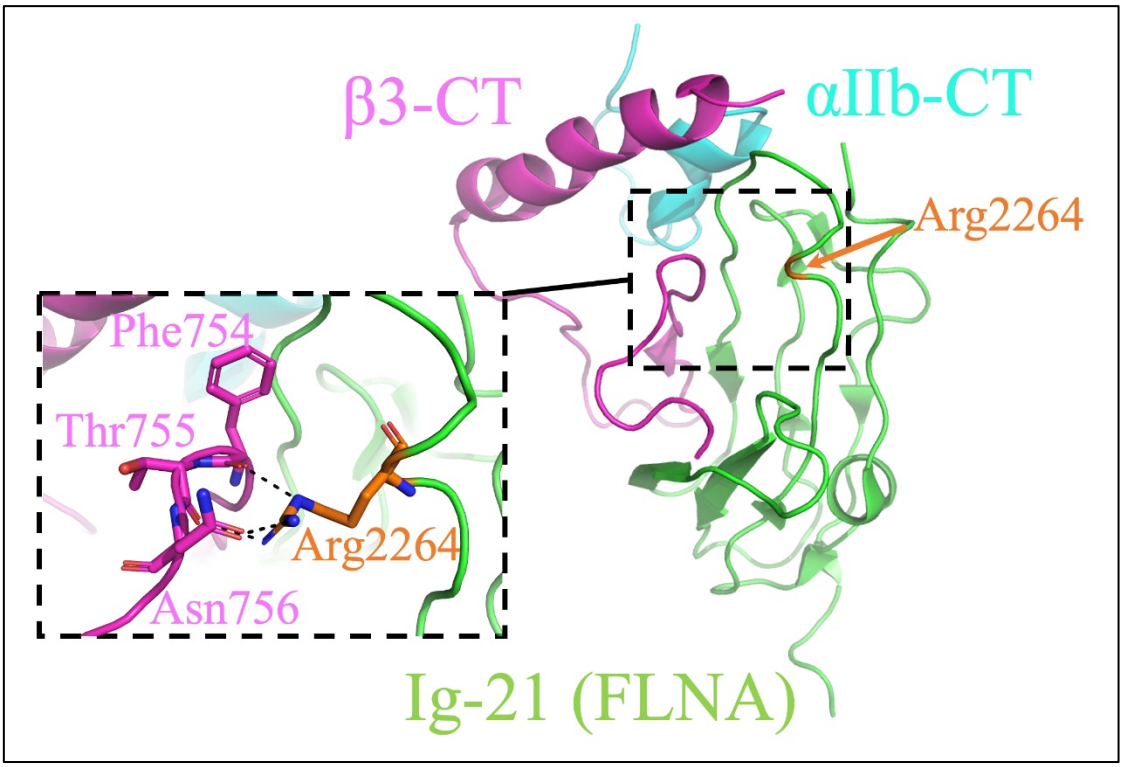

Figure S3: Nuclear magnetic resonance (NMR) structure of the domain 21 of Filamin A (FLNA) in complex with β3-C-terminal (CT) and αIIb-CT peptide (PDB code: 2MTP). The structures of the actin-binding domain and Ig-like domains of the FLNA dimer are known from nuclear magnetic resonance and X-ray crystallography studies.[1] The represented structure was obtained from NMR studies. The ribbon diagram shows the 16th conformer of the Ig-21-αIIbβ3 CT complex with Ig-21 in green and key residue Arg2264 in orange, β3-CT in magenta, and αIIb-CT in cyan. The inset shows a zoom-in of the structure with contact residues Phe754, Thr755, and Asn756 of β3-CT, and Arg2264 of Ig-21. The black dashed lines show 3 hydrogen bonds between contact residues. Arg2264 is involve in transient but strong interaction with integrin αIIbβ3.[2]